The stability of multiple, high power, active front end voltage sourced converters when connected to wind farm collector systems.

Paul Brogan – Siemens Wind Power.

Abstract:

In much of the published analysis of the operation of active front end voltage sourced converters connected to power systems, the network is represented as a simple resistive inductive circuit. However real, multiple turbine, wind park collector systems have significant MV collector cabling and/or overhead lines, and depending on the wind farm, HV cabling which add distributed capacitance and so create resonances which interact with the active front end (network bridge) closed loop current control. The characteristics of these resonances, and hence the stability margins of the closed loop systems, are dependent on the number of collector cables in service, the system fault level, the number of turbines connected, power factor correction equipment, as well as the frequency dependency of such components. This can represent a significant range of operating conditions.

This paper presents the multiple methods by which the stability of such systems can be assessed using actual wind farm data, and then examines the stability implications when standard current controllers are used, such as those presented in much of the published literature.

It will be shown that such systems can be robustly controlled to meet the demanding transient and steady state stability requirements required from modern power converters within such applications and how, through the use of the these techniques, large numbers of wind turbines operating on relatively low fault level supplies can be integrated into the power supply network.

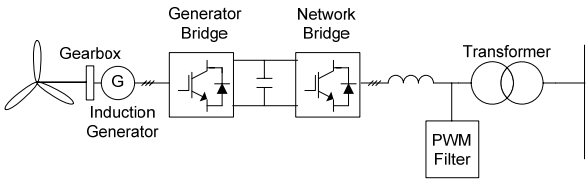

Figure 1. Variable speed wind turbine with fully rated converters.

Introduction.

Variable speed wind turbines with fully rated converters, as shown in Figure 1, have the advantage of both variable speed control of the generator and full dynamic control of the network side current(s). This control of both the positive and negative sequence fundamental frequency components of the network side current, permits full reactive power support during both symmetric and asymmetric grid faults, as well as steady state power control and AC voltage regulation.

Typically the control of the network bridge current is achieved by using dual synchronously rotating reference frames [1, 2] the typical arrangement of which is shown in Figure 2.

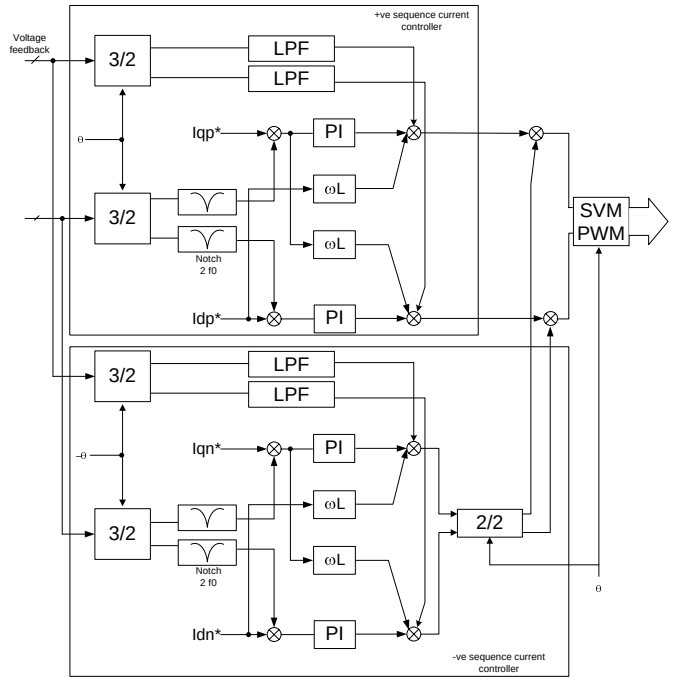

Figure 2. Structure of a typical dual current controller

Within such a controller, which would typically be implemented digitally in a microprocessor or DSP, the positive sequence current is controlled within the positive sequence synchronous reference frame (SRF) and the negative sequence current controlled within the negative SRF. In the steady state the reference and feedback signals are DC quantities and via the action of the respective proportional plus integral (PI) controllers the steady state error of both the positive and negative sequence DQ axis current components is zero. Such a control arrangement also includes a voltage feed-forward component, typically of the turbine LV busbar voltage, which also makes a 'contribution' to the total PWM output voltage as shown in Figure 2.

Such DQ axis current controllers are robust and used in many industrial applications, however since such controllers are predominantly implemented digitally, there will be a point where the phase lag introduced by the controller reaches -180°, with finite gain due to the proportional gain term. In most industrial applications to date the electrical system will have been 'stiff', and not have had significant gain at higher frequencies, or frequencies close to the point where the controller phase crosses -180°. However within wind farm collector systems local cable or other capacitances have been found to cause series resonances which can provide significant 'plant' gain at higher frequencies. The combination of the significant numbers of high power network connected, current controlled converters and the presence of significant plant gain, is investigated in this paper.

Single turbine frequency domain model

In order to investigate the stability of such systems a frequency domain model of the combined converter current controller and the electrical system is required. A simplified representation of the system is shown in Figure 3, within which the control structure of Figure 2 is represented by the frequency dependent complex gains Vg(s) and Ig(s).

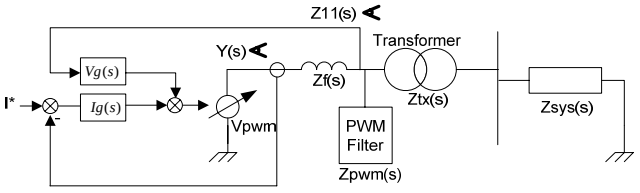

Figure 3. Single line simplification of the network bridge

The following definitions are made regarding Figure 3.

$$Y(s) = \frac{1}{Zf(s) + \left(Zsys(s) + Ztx(s)\right) // \, Zpwm(s)} \qquad \textbf{(1)}$$

$$Z11(s) = \left(Zsys(s) + Ztx(s)\right) // \, Zpwm(s) \qquad \textbf{(2)}$$

Vg(s) The complex gain of both the +ve and –ve sequence voltage feed-forward contribution to Vpwm.

Ig(s) The complex gain of the combined +ve and –ve sequence current controller's contribution to Vpwm.

Y(s) The total complex admittance as viewed from the terminals of the network power converter

Z11(s) The complex impedance looking into the electrical system from the point at which the voltage is measured.

Zsys(s) The complex impedance of the MV and HV wind farm collector system. This includes the MV collector system, Park Transformer and HV system impedances.

Vpwm Ideal, controlled voltage source, representation of the PWM modulator.

Z(s) The complex impedance of the filter reactor.

Ztx(s) The complex impedance of the transformer.

It should be noted that $Vg(s)$ and $Ig(s)$ both include the complete characteristics of these respective control loops including anti-aliasing filters, Analog to Digital converters, the discrete delay associated with the microprocessor control and realisation of the voltages via the PWM modulator.

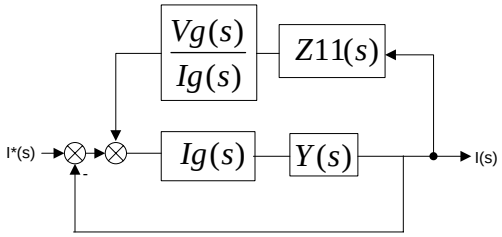

Figure 4. Network bridge current control loop

After simplification [3] the open loop gain of the complete network bridge current controller can be derived from Figure 4. The open loop gain of this single turbine system can be derived as:

$$G_{o/l}(s) = \frac{Ig(s)Y(s)}{1 - Vg(s)Z11(s)Y(s)} \qquad \textbf{(3)}$$

It is interesting to note that on the numerator the gain is defined as the current controller gains multiplied by the total system admittance. The voltage feed-forward contribution appears on the denominator and that an infinite gain situation can exist for cases where the controller voltage loop gain satisfies equation (4). Thus for steady state operation the voltage feed-forward is heavily filtered, and $Vg(s) \approx 0$. It can be shown that this infinite gain condition is dependent on the electrical system parameters and for this reason it is believed that the current control loop cannot be universally decoupled from electrical system by the use of voltage feed-forward signals within the controller.

$$Vg(s) = \frac{1}{Z11(s)Y(s)} \qquad \textbf{(4)}$$

Using equation 3 the open loop gain and phase of a simple, single turbine system with a RL representation of the collector system, Zsys(s), can be calculated. This is shown in the Bode plot of Figure 5 (green) and as can be seen from the Nyquist plot of Figure 6 the system is stable.

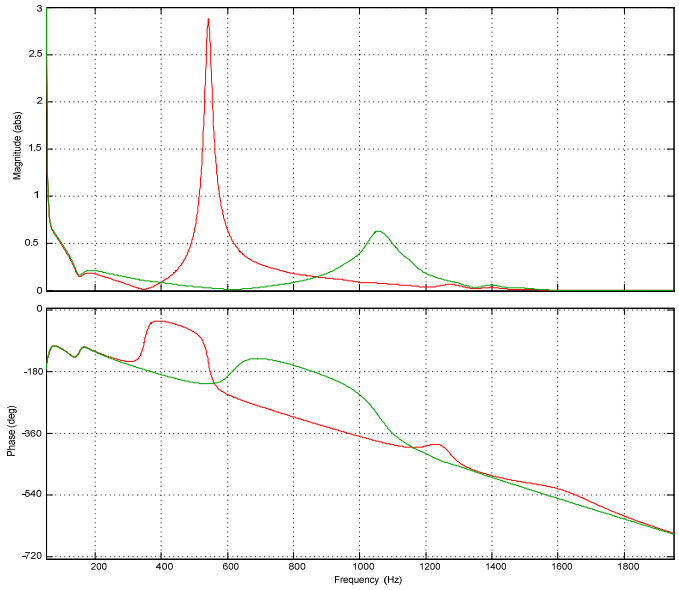

Figure 5. Open loop Bode plot with cable capacitance (red) and without (green)

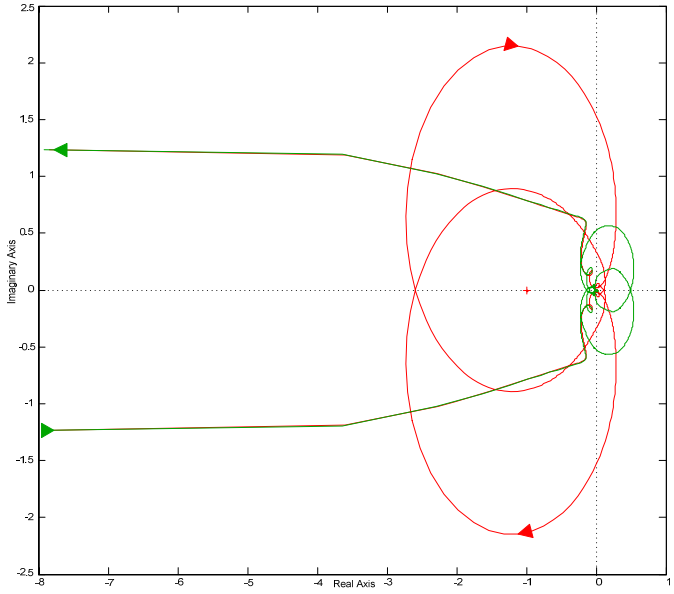

Figure 6. Nyquist plot with cable capacitance (red) and without (green).

However such a simplification is unrealistic and a more thorough examination of the stability is required, where the collector system capacitances are included. The open loop gain of the single turbine system with the cable capacitances included is shown in the Bode plot of Figure 5 (red). The effect of the series resonance is a significantly higher gain close to 550Hz, which the Nyquist plot of Figure 6 shows will result in an unstable system.

Using equation (3) it is possible to plot the open loop gain and phase response of a single turbine system, and assess the stability margins. It is however equally important to assess the stability of an N turbine wind farm, where multiple current controllers are in operation, as in the case in a real wind farm.

Multi turbine frequency domain model

Consider an example wind farm with N turbines (7) connected on C collector radials (3) as shown in Figure 7. This is a very typical arrangement used in many systems installed to date.

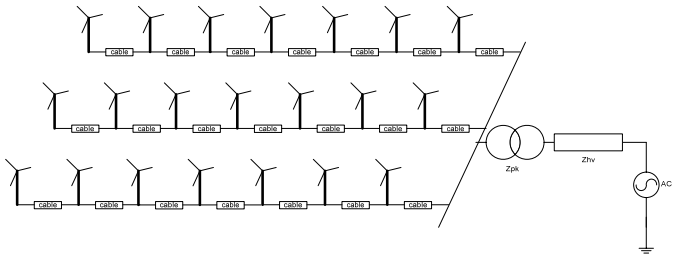

Figure 7. Example wind farm collector system

In order to make a realistic stability assessment of the system in the frequency domain the cable capacitances of the collector system must be included in Zsys(s) shown in Figure 3. It has also been found that a reasonable representation of an N turbine radial is that the N turbines can be represented as a single lumped equivalent as shown in Figure 8. The critical parameter within this lumped model of the MV collector cables is that the equivalent capacitance represents that of the complete distributed radial cable capacitance. The power components within the lumped turbine model(s) are all scaled by N appropriately, as are the current controller gains.

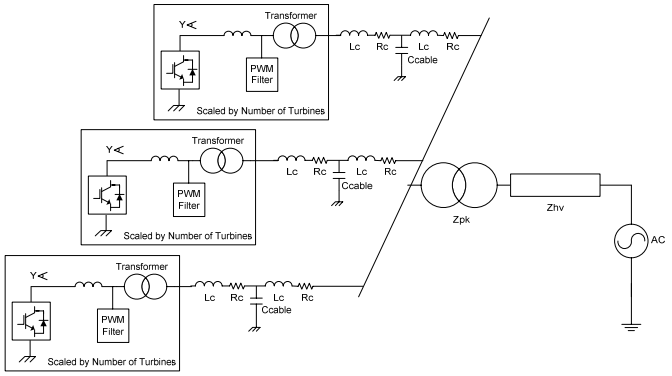

Figure 8. Simplified model of a 3 radial wind farm

$$G_{o/l}(s) = \frac{I_g(s)}{Z_f(s) + \left(Z_{tx}(s) + NZ_{sys}(s)\right)\left(1 - V_g(s)\right)} \quad \textbf{(5)}$$

Equation (5) gives the open loop gain of an N turbine system on one of the 3 radials shown in Figure 7. A further approximation is that the C collector radials (in this case 3) can be paralleled giving a single model which represents the N turbine, C collector system of Figure 7, as shown in Figure 9. This equivalent circuit together with equation (5) and (6) allow the open loop gain to be calculated for an N turbine, C collector farm as shown in equation (7).

$$Z_{sys}(s) = Z_{hv}(s) + Z_{pk}(s) + \frac{Z_c(s)}{C} \quad \textbf{(6)}$$

Substituting (6) into (5) gives

$$G_{o/l}(s) = \frac{I_g(s)}{Z_{sfe}(s) + \left(Z_{tx}(s) + NZ_{hv}(s) + NZ_{pk}(s) + \frac{NZ_c(s)}{C}\right)\left(1 - V_g(s)\right)} \quad \textbf{(7)}$$

With the electrical system, represented in the frequency domain via the appropriate (frequency dependent) impedances, it is then possible to plot the open loop gain and phase characteristics, using equation (7), for all combinations of number of turbines, number of collector cables, HV system fault level and/or HV cables. For a given system fault level a family of such bode plots can then be drawn for, in the case shown, each combination of 1 to 3 collector cables and 1 to N turbines. This is shown in Figure 10 where red is with 3 collector cables, green 2, and blue 1 collector cable in service. What is interesting to note is the combination of the high gain associated with the low impedance (high admittance) of the electrical system can result in a situation where the gain is greater than unity and the phase less than -180°, and hence an unstable system exists. There is also a significant change in the resonant frequency depending on the number of collector cables in service, and (smaller) changes in resonant frequency associated with the number of turbines running. This technique shows that in a real wind farm collector system that the simplification that the electrical system can be modeled as a simple RL network is simply not valid as the actual site conditions are significantly more demanding.

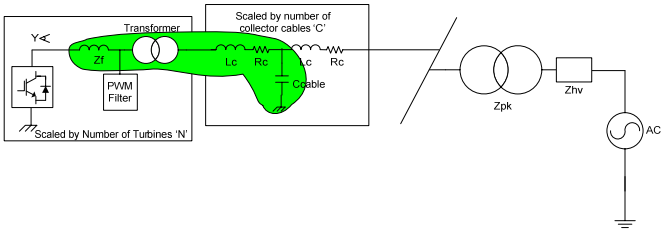

Figure 9. Single turbine equivalent of Wind farm

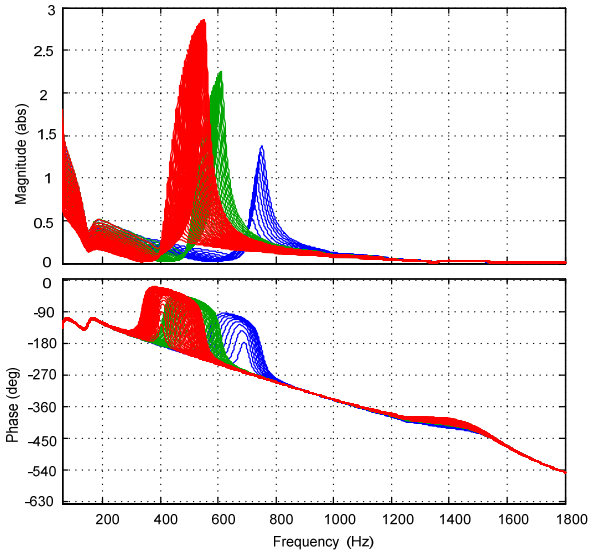

Figure 10. Open loop Bode plot for a 3 collector wind farm

The high admittance which results in the open loop gain exceeding unity is a consequence of the low system impedance or high system admittance Y (as viewed from the terminals of the converter) caused by the series resonance between the shunt cable capacitance (Ccable), turbine transformer (Ztx) and input line reactor (Zf) as shown highlighted in Figure 9. The PWM filter, although included in the frequency domain analysis, does not have a significant effect on system stability and has been omitted from equations (5),(6) and (7) for clarity. The PWM filter is strongly influential in attenuating switching frequency harmonics which are at a much higher frequency that the resonance frequencies associated with the RLC characteristics of the collector network and network bridge power converter inductive components.

The effect of the open loop gain shown in Figure 10, is better seen on a Nyquist plot, Figure 11, where the Nyquist contour is plotted for the 1 to N turbines on the 1 to 3 collector system. Clearly multiple combinations of collector cables and number of turbines exists where the Nyquist contour encircles the point [-1,0] and indicating that system will be, and was, unstable.

Using this frequency domain method a series of such frequency domain plots can be made to investigate the stability of any system across, for example, a range of system fault levels, connection of MV or LV power factor correction capacitors or filters, series compensated transmission lines, and or HV cables or transmission lines.

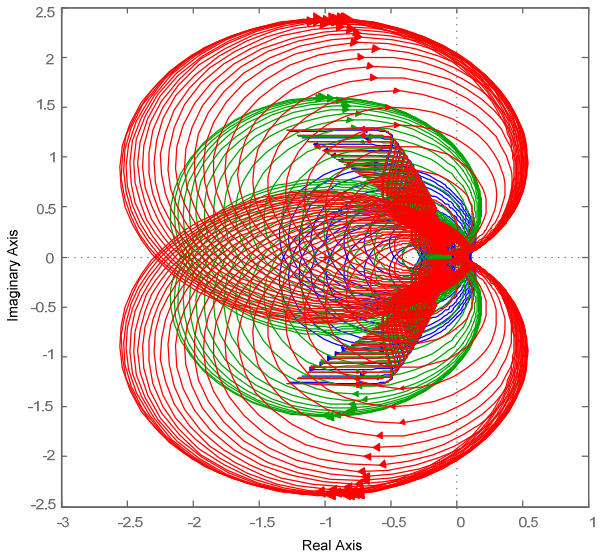

Figure 11. Nyquist contours for a 3 collector wind farm

Correlation to site measurements

Whilst the above analysis is very plausible in simulation, some correlation with actual site conditions is desirable, to justify the simplifications made regarding, particularly, the equivalent circuit(s) used. The Nyquist plot shown in Figure 12, shows the multiple open loop frequency responses which result from 2 collector cables and 1 to 2/3 of the total of N turbines in service.

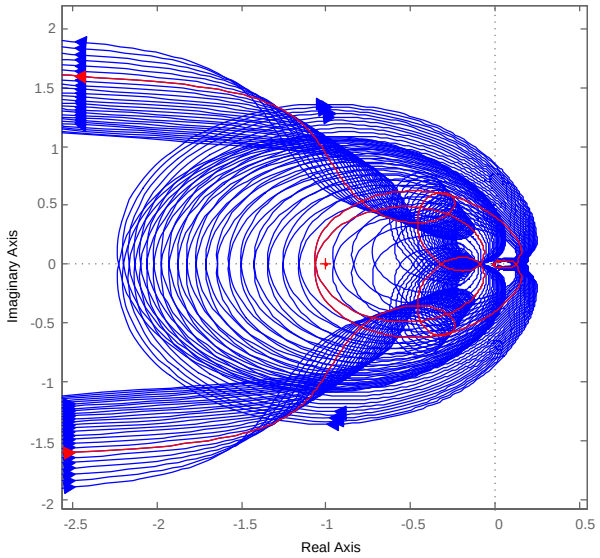

Figure 12. Nyquist plot of 1 – N turbines with 2 MV collector cables connected. 7 turbines case shown in red.

The contour shown in red is with 7 turbines in operation, which, on the actual wind farm, is the point at which the voltage began to oscillate and the current control went unstable. Similar correlation was made with other combinations of turbines and collector cables. It was found however that there is a dependency on the background damping provided by the HV system and this can be difficult to ascertain. Significant variations in the damping provided by the HV system were calculated based on site measurements and correlation to the frequency domain model.

Robust control

In order to resolve this situation and provide a robust controller arrangement that removes dependency on system damping, sensitivity to number of turbines, number of collectors or tolerance on system parameters such as fault level, a modification to the controller shown in Figure 2 was proposed by Siemens. For convenience of operation, such a controller must continue to operate autonomously from the other turbine current controllers, without knowledge of the number of turbines in operation, or any information on system impedance, and have sufficient current loop bandwidth to provide full symmetric and asymmetric fault ride through capability. It is also highly desirable that such a controller is universal and that the controller gains do not need to be calculated on a site specific basis.

The Bode plot of Figure 10 clearly shows the increased gain between 400Hz and 800Hz, due to the series resonance associated with the collector cable capacitances. In order to stabilise such systems an additional notch filter in the current feedback has been implemented as shown in Figure 13. These are wideband digital notch filters, implemented in the positive and negative sequence DQ axis current feedback signal paths. Such filters provide significant attenuation to the gain introduced to the control system by the 'plant', the electrical system resonance(s), for all combinations of collector cables and turbines in operation.

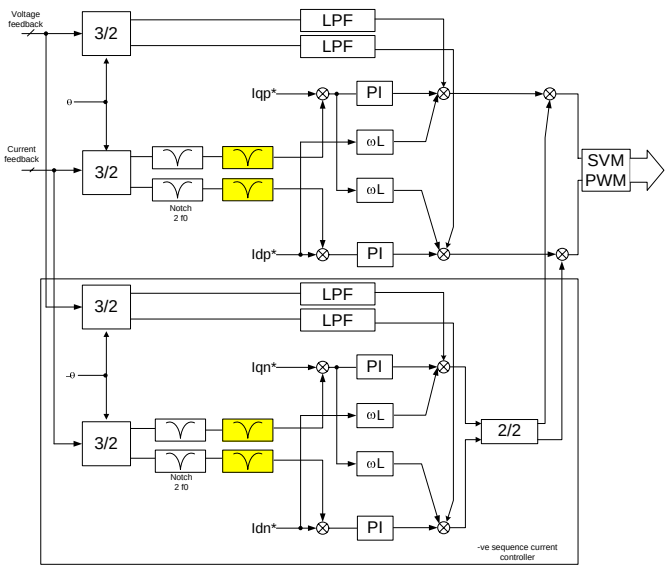

Figure 13. Improved dual vector current controller

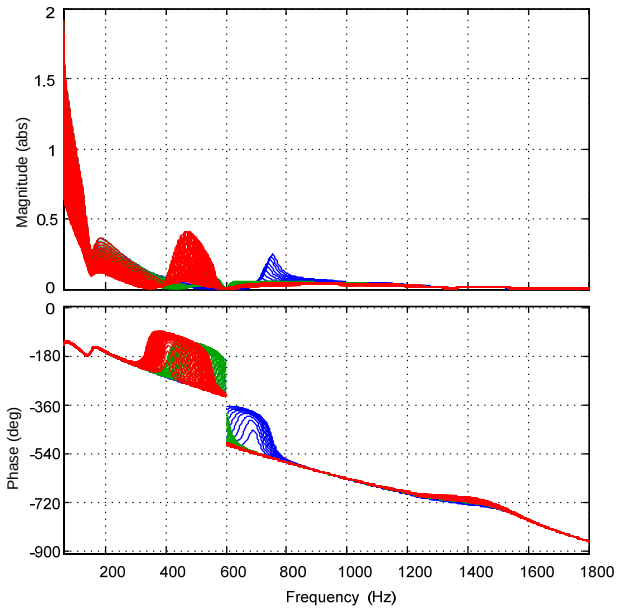

Figure 14. Bode plot with stabilising notch filters.

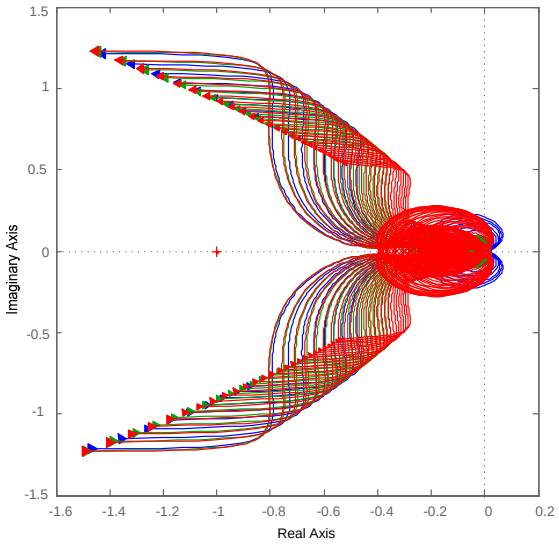

Figure 15. Nyquist plot with stabilising notch filters.

The open loop gain of the system with the additional notch filter is shown in the Bode plot of Figure 14 along with the corresponding Nyquist plot shown in Figure 15. This shows that the system is now stable for all combinations of turbines and collector cables.

Validation of the stability margins achieved with the above technique was carried out on a wind farm. This was achieved by increasing the current loop gain within the controller with and without the notch filters enabled until the system went unstable and the turbine protection system shut down the turbine. With knowledge of the system conditions and the controller gains/configurations this was then correlated back to the frequency domain model which showed good agreement with the site measurements.

When designing the notch filter the bandwidth, centre frequency and attenuation (of the notch filter) is determined from the particular wind farm configuration in order to respect the phase margin requirements during the worst case conditions.

Conclusions

A method by which a frequency domain stability assessment of the connection of multiple high power network bridge current control converters has been presented. Such current control systems have been found to interact with the electrical collector systems found in wind farms, and a method to stabilise such systems proposed. Siemens Wind Power together with their customers have performed many such stability studies to ensure stability and as a result have many different wind farms operating with hundreds of turbines in these demanding electrical systems using the control techniques presented in this paper.

References

1. Dual Current Control Scheme for PWM Converter Under Unbalanced Input Voltage Conditions. Hong-seok Song, Kwanghee Nam. IEEE Trans Ind. Electronics, Vol. 46, No 5, Oct 1999. pp 953-959.
2. Transient Operation of Grid_connected Voltage Source Converter Under Unbalanced Voltage Conditions. G. Saccomando, J. Svensson. IEEE 2001, pp 2419-2424
3. Morris Driels. Linear Control systems Engineering, McGraw-Hill International Editions 1996, page 26.
4. Tuning of Control Loops for Grid Connected Voltage Sourced Converters. JA Suul, M Molinas, T Underland. 2nd PECon 08, Dec. 1-3, 2008. Malaysia. pp 797-802.